# Study of ψ(3686)→ωKK[over ¯]π decays

M. Ablikim *et al.* (BESIII Collaboration)

Phys. Rev. D **87**, 092006 — Published 20 May 2013

DOI: 10.1103/PhysRevD.87.092006

# Study of $\psi(3686) \to \omega K \bar{K} \pi$ decays


M. Ablikim[1], M. N. Achasov[6], O. Albayrak[3], D. J. Ambrose[39], F. F. An[1], Q. An[40], J. Z. Bai[1], R. Baldini Ferroli[17A], Y. Ban[26], J. Becker[2], J. V. Bennett[16], M. Bertani[17A], J. M. Bian[38], E. Boger[19,a], O. Bondarenko[20], I. Boyko[19], R. A. Briere[3], V. Bytev[19], H. Cai[44], X. Cai[1], O. Cakir[34A], A. Calcaterra[17A], G. F. Cao[1], S. A. Cetin[34B], J. F. Chang[1], G. Chelkov[19,a], G. Chen[1], H. S. Chen[1], J. C. Chen[1], M. L. Chen[1], S. J. Chen[24], X. Chen[26], Y. B. Chen[1], H. P. Cheng[14], Y. P. Chu[1], D. Cronin-Hennessy[38], H. L. Dai[1], J. P. Dai[1], D. Dedovich[19], Z. Y. Deng[1], A. Denig[18], I. Denysenko[19,b], M. Destefanis[43A,43C], W. M. Ding[28], Y. Ding[22], L. Y. Dong[1], M. Y. Dong[1], S. X. Du[46], J. Fang[1], S. S. Fang[1], L. Fava[43B,43C], C. Q. Feng[40], P. Friedel[2], C. D. Fu[1], J. L. Fu[24], Y. Gao[33], C. Geng[40], K. Goetzen[7], W. X. Gong[1], W. Gradl[18], M. Greco[43A,43C], M. H. Gu[1], Y. T. Gu[9], Y. H. Guan[36], N. Guler[34C], A. Q. Guo[25], L. B. Guo[23], T. Guo[23], Y. P. Guo[25], Y. L. Han[1], F. A. Harris[37], K. L. He[1], M. He[1], Z. Y. He[25], T. Held[2], Y. K. Heng[1], Z. L. Hou[1], C. Hu[23], H. M. Hu[1], J. F. Hu[35], T. Hu[1], G. M. Huang[4], G. S. Huang[40], J. S. Huang[12], L. Huang[1], X. T. Huang[28], Y. Huang[24], Y. P. Huang[1], T. Hussain[42], C. S. Ji[40], Q. Ji[1], Q. P. Ji[25], X. B. Ji[1], X. L. Ji[1], L. L. Jiang[1], X. S. Jiang[1], J. B. Jiao[28], Z. Jiao[14], D. P. Jin[1], S. Jin[1], F. F. Jing[33], N. Kalantar-Nayestanaki[20], M. Kavatsyuk[20], B. Kopf[2], M. Kornicer[37], W. Kuehn[35], W. Lai[1], J. S. Lange[35], M. Leyhe[2], C. H. Li[1], Cheng Li[40], Cui Li[40], D. M. Li[46], F. Li[1], G. Li[1], H. B. Li[1], J. C. Li[1], K. Li[10], Lei Li[1], Q. J. Li[1], S. L. Li[1], W. D. Li[1], W. G. Li[1], X. L. Li[28], X. N. Li[1], X. Q. Li[25], X. R. Li[27], Z. B. Li[32], H. Liang[40], Y. F. Liang[30], Y. T. Liang[35], G. R. Liao[33], X. T. Liao[1], D. Lin[11], B. J. Liu[1], C. L. Liu[3], C. X. Liu[1], F. H. Liu[29], Fang Liu[1], Feng Liu[4], H. Liu[1], H. B. Liu[9], H. H. Liu[13], H. M. Liu[1], H. W. Liu[1], J. P. Liu[44], K. Liu[33], K. Y. Liu[22], Kai Liu[36], P. L. Liu[28], Q. Liu[36], S. B. Liu[40], X. Liu[21], Y. B. Liu[25], Z. A. Liu[1], Zhiqiang Liu[1], Zhiqing Liu[1], H. Loehner[20], G. R. Lu[12], H. J. Lu[14], J. G. Lu[1], Q. W. Lu[29], X. R. Lu[36], Y. P. Lu[1], C. L. Luo[23], M. X. Luo[45], T. Luo[37], X. L. Luo[1], M. Lv[1], C. L. Ma[36], F. C. Ma[22], H. L. Ma[1], Q. M. Ma[1], S. Ma[1], T. Ma[1], X. Y. Ma[1], F. E. Maas[11], M. Maggiora[43A,43C], Q. A. Malik[42], Y. J. Mao[26], Z. P. Mao[1], J. G. Messchendorp[20], J. Min[1], T. J. Min[1], R. E. Mitchell[16], X. H. Mo[1], H. Moeini[20], C. Morales Morales[11], K. Moriya[16], N. Yu. Muchnoi[6], H. Muramatsu[39], Y. Nefedov[19], C. Nicholson[36], I. B. Nikolaev[6], Z. Ning[1], S. L. Olsen[27], Q. Ouyang[1], S. Pacetti[17B], J. W. Park[27], M. Pelizaeus[2], H. P. Peng[40], K. Peters[7], J. L. Ping[23], R. G. Ping[1], R. Poling[38], E. Prencipe[18], M. Qi[24], S. Qian[1], C. F. Qiao[36], L. Q. Qin[28], X. S. Qin[1], Y. Qin[26], Z. H. Qin[1], J. F. Qiu[1], K. H. Rashid[42], G. Rong[1], X. D. Ruan[9], A. Sarantsev[19,c], H. Sazak[34A], B. D. Schaefer[16], M. Shao[40], C. P. Shen[37,d], X. Y. Shen[1], H. Y. Sheng[1], M. R. Shepherd[16], W. M. Song[1], X. Y. Song[1], S. Spataro[43A,43C], B. Spruck[35], D. H. Sun[1], G. X. Sun[1], J. F. Sun[12], S. S. Sun[1], Y. J. Sun[40], Y. Z. Sun[1], Z. J. Sun[1], Z. T. Sun[40], C. J. Tang[30], X. Tang[1], I. Tapan[34C], E. H. Thorndike[39], D. Toth[38], M. Ullrich[35], I. Uman[34B], G. S. Varner[37], B. Q. Wang[26], D. Wang[26], D. Y. Wang[26], K. Wang[1], L. L. Wang[1], L. S. Wang[1], M. Wang[28], P. Wang[1], P. L. Wang[1], Q. J. Wang[1], S. G. Wang[26], X. F. Wang[33], X. L. Wang[40], Y. D. Wang[17A], Y. F. Wang[1], Y. Q. Wang[18], Z. Wang[1], Z. G. Wang[1], Z. Y. Wang[1], D. H. Wei[8], J. B. Wei[26], P. Weidenkaff[18], Q. G. Wen[40], S. P. Wen[1], M. Werner[35], U. Wiedner[2], L. H. Wu[1], N. Wu[1], S. X. Wu[40], W. Wu[25], Z. Wu[1], L. G. Xia[33], Y. X Xia[15], Z. J. Xiao[23], Y. G. Xie[1], Q. L. Xiu[1], G. F. Xu[1], G. M. Xu[26], Q. J. Xu[10], Q. N. Xu[36], X. P. Xu[31], Z. R. Xu[40], F. Xue[4], Z. Xue[1], L. Yan[40], W. B. Yan[40], Y. H. Yan[15], H. X. Yang[1], Y. Yang[4], Y. X. Yang[8], H. Ye[1], M. Ye[1], M. H. Ye[5], B. X. Yu[1], C. X. Yu[25], H. W. Yu[26], J. S. Yu[21], S. P. Yu[28], C. Z. Yuan[1], Y. Yuan[1], A. A. Zafar[42], A. Zallo[17A], S. L. Zang[24], Y. Zeng[15], B. Zengin[34A], B. X. Zhang[1], B. Y. Zhang[1], C. Zhang[24], C. C. Zhang[1], D. H. Zhang[1], H. H. Zhang[32], H. Y. Zhang[1], J. Q. Zhang[1], J. W. Zhang[1], J. Y. Zhang[1], J. Z. Zhang[1], LiLi Zhang[15], R. Zhang[36], S. H. Zhang[1], X. J. Zhang[1], X. Y. Zhang[28], Y. Zhang[1], Y. H. Zhang[1], Z. P. Zhang[40], Z. Y. Zhang[44], Zhenghao Zhang[4], G. Zhao[1], H. S. Zhao[1], J. W. Zhao[1], K. X. Zhao[23], Lei Zhao[40], Ling Zhao[1], M. G. Zhao[25], Q. Zhao[1], S. J. Zhao[46], T. C. Zhao[1], X. H. Zhao[24], Y. B. Zhao[1], Z. G. Zhao[40], A. Zhemchugov[19,a], B. Zheng[41], J. P. Zheng[1], Y. H. Zheng[36], B. Zhong[23], L. Zhou[1], X. Zhou[44], X. K. Zhou[36], X. R. Zhou[40], C. Zhu[1], K. Zhu[1], K. J. Zhu[1], S. H. Zhu[1], X. L. Zhu[33], Y. C. Zhu[40], Y. M. Zhu[25], Y. S. Zhu[1], Z. A. Zhu[1], J. Zhuang[1], B. S. Zou[1], J. H. Zou[1]

(BESIII Collaboration)

[1] *Institute of High Energy Physics, Beijing 100049, People's Republic of China*
[2] *Bochum Ruhr-University, D-44780 Bochum, Germany*
[3] *Carnegie Mellon University, Pittsburgh, Pennsylvania 15213, USA*
[4] *Central China Normal University, Wuhan 430079, People's Republic of China*
[5] *China Center of Advanced Science and Technology, Beijing 100190, People's Republic of China*
[6] *G.I. Budker Institute of Nuclear Physics SB RAS (BINP), Novosibirsk 630090, Russia*
[7] *GSI Helmholtzcentre for Heavy Ion Research GmbH, D-64291 Darmstadt, Germany*
[8] *Guangxi Normal University, Guilin 541004, People's Republic of China*
[9] *GuangXi University, Nanning 530004, People's Republic of China*
[10] *Hangzhou Normal University, Hangzhou 310036, People's Republic of China*
[11] *Helmholtz Institute Mainz, Johann-Joachim-Becher-Weg 45, D-55099 Mainz, Germany*
[12] *Henan Normal University, Xinxiang 453007, People's Republic of China*
[13] *Henan University of Science and Technology, Luoyang 471003, People's Republic of China*
[14] *Huangshan College, Huangshan 245000, People's Republic of China*
[15] *Hunan University, Changsha 410082, People's Republic of China*
[16] *Indiana University, Bloomington, Indiana 47405, USA*
[17] *(A)INFN Laboratori Nazionali di Frascati, I-00044, Frascati, Italy; (B)INFN and University of Perugia, I-06100, Perugia, Italy*
[18] *Johannes Gutenberg University of Mainz, Johann-Joachim-Becher-Weg 45, D-55099 Mainz, Germany*

[19] *Joint Institute for Nuclear Research, 141980 Dubna, Moscow region, Russia*
[20] *KVI, University of Groningen, NL-9747 AA Groningen, The Netherlands*
[21] *Lanzhou University, Lanzhou 730000, People's Republic of China*
[22] *Liaoning University, Shenyang 110036, People's Republic of China*
[23] *Nanjing Normal University, Nanjing 210023, People's Republic of China*
[24] *Nanjing University, Nanjing 210093, People's Republic of China*
[25] *Nankai University, Tianjin 300071, People's Republic of China*
[26] *Peking University, Beijing 100871, People's Republic of China*
[27] *Seoul National University, Seoul, 151-747 Korea*
[28] *Shandong University, Jinan 250100, People's Republic of China*
[29] *Shanxi University, Taiyuan 030006, People's Republic of China*
[30] *Sichuan University, Chengdu 610064, People's Republic of China*
[31] *Soochow University, Suzhou 215006, People's Republic of China*
[32] *Sun Yat-Sen University, Guangzhou 510275, People's Republic of China*
[33] *Tsinghua University, Beijing 100084, People's Republic of China*
[34] *(A)Ankara University, Dogol Caddesi, 06100 Tandogan, Ankara, Turkey; (B)Dogus University, 34722 Istanbul, Turkey; (C)Uludag University, 16059 Bursa, Turkey*
[35] *Universitaet Giessen, D-35392 Giessen, Germany*
[36] *University of Chinese Academy of Sciences, Beijing 100049, People's Republic of China*
[37] *University of Hawaii, Honolulu, Hawaii 96822, USA*
[38] *University of Minnesota, Minneapolis, Minnesota 55455, USA*
[39] *University of Rochester, Rochester, New York 14627, USA*
[40] *University of Science and Technology of China, Hefei 230026, People's Republic of China*
[41] *University of South China, Hengyang 421001, People's Republic of China*
[42] *University of the Punjab, Lahore-54590, Pakistan*
[43] *(A)University of Turin, I-10125, Turin, Italy; (B)University of Eastern Piedmont, I-15121, Alessandria, Italy; (C)INFN, I-10125, Turin, Italy*
[44] *Wuhan University, Wuhan 430072, People's Republic of China*
[45] *Zhejiang University, Hangzhou 310027, People's Republic of China*
[46] *Zhengzhou University, Zhengzhou 450001, People's Republic of China*

[a] *Also at the Moscow Institute of Physics and Technology, Moscow 141700, Russia*
[b] *On leave from the Bogolyubov Institute for Theoretical Physics, Kiev 03680, Ukraine*
[c] *Also at the PNPI, Gatchina 188300, Russia*
[d] *Present address: Nagoya University, Nagoya 464-8601, Japan*

Based on 106 million $\psi(3686)$ events collected with the BESIII detector at the BEPCII, the decay $\psi(3686) \to \omega K\bar{K}\pi$ is studied. Enhancements around 1.44 GeV/$c^2$ and the $f_1(1285)$ are observed in the mass spectrum of $K\bar{K}\pi$, and the corresponding branching fraction (upper limit) is measured, as well as the branching fractions of $\psi(3686) \to \omega K^{*+}K^- + c.c.$ and $\psi(3686) \to \omega \bar{K}^{*0}K^0 + c.c.$, all for the first time.

PACS numbers: 13.85.Hd, 25.75Gz

## I. INTRODUCTION

Charmonium decays play an important role in the study of the strong interactions. The $\psi(3686)$, which was the second charmonium state discovered [1], has been extensively studied both experimentally [2–6] and theoretically [7–10]. Perturbative QCD [11, 12] predicts that the partial widths for $J/\psi$ and $\psi(3686)$ decays into an exclusive hadronic state $h$ are proportional to the squares of the $c\bar{c}$ wave-function overlap at zero quark separation, which are well determined from the leptonic widths. Since the strong coupling constant, $\alpha_s$, is not very different at the $J/\psi$ and $\psi(3686)$ masses, it is expected that the $J/\psi$ and $\psi(3686)$ branching fractions of any exclusive hadronic state $h$ are related by

$$Q_h = \frac{\mathcal{B}(\psi(3686) \to h)}{\mathcal{B}(J/\psi \to h)} \cong \frac{\mathcal{B}(\psi(3686) \to e^+e^-)}{\mathcal{B}(J/\psi \to e^+e^-)} \cong 12\%.$$

This relation defines the "12% rule", which works reasonably well for many specific decay modes. A large violation of this rule was observed by later experiments [3, 4, 6], particularly in the $\rho\pi$ decay. Recent reviews [9, 10] of relevant theories and experiments conclude that current theoretical explanations are unsatisfactory. Clearly, more experimental results are also desirable.

In addition to test "12% rule", the study of the decays $\psi(3686)$ $(J/\psi) \to \{\gamma, \omega, \phi\}K\bar{K}\pi$ provides valuable information to understand the nature of the pseudoscalar gluonium candidate around 1.44 GeV/$c^2$, the so-called $E/\iota(1440)$, was first observed in $p\bar{p}$ annihilation in 1967 [13]. Studies in different decay modes revealed the existence of two resonant structures, the $\eta(1405)$ and the $\eta(1475)$ [14]. The $\eta(1475)$ could be the first radial excitation of $\eta^{'}(958)$. The L3 measurements of the $K\bar{K}\pi$ and $\eta\pi^+\pi^-$ decays in photon-photon fusion suggest that the $\eta(1405)$ has a large gluonic content [15]. However, CLEO with a five times larger data sample did not confirm the L3 results, but their upper limits are still consistent with the glueball and the radial excitation hypotheses for the $\eta(1405)$ and $\eta(1475)$ [16].

In this paper, the first observation of enhancements at around 1.44 GeV/$c^2$ and at the $f_1(1285)$ resonance in the mass spectrum of $K\bar{K}\pi$ ($K^0_S K^+\pi^- + c.c.$ and $K^+K^-\pi^0$) produced in $\psi(3686) \to \omega K\bar{K}\pi$ and the measurements of the corresponding branching fractions (upper limits) are reported. In addition, the branching fractions of $\psi(3686) \to \omega K^{*+}K^- + c.c.$ and $\psi(3686) \to \omega\bar{K}^{*0}K^0 + c.c.$ are also measured for the first time. The analysis reported here is based on $1.06 \times 10^8 \psi(3686)$ events collected with the BESIII detector at BEPCII.

## II. BESIII DETECTOR

BEPCII/BESIII [17] is a major upgrade of the BESII experiment at the BEPC accelerator [18, 19] for studies of hadron spectroscopy, charmonium physics, and $\tau$-charm physics [20]. The design peak luminosity of the double-ring $e^+e^-$ collider, BEPCII, is $10^{33}$ cm$^{-2}s^{-1}$ at a beam current of 0.93 A at the $\psi(3770)$ peak. The BESIII detector with a geometrical acceptance of 93% of $4\pi$, consists of the following main components: 1) a small-celled, helium-based main draft chamber (MDC) with 43 layers. The average single wire resolution is 135 $\mu m$, and the momentum resolution for 1 GeV/$c$ charged particles in a 1 T magnetic field is 0.5%; 2) an electromagnetic calorimeter (EMC) made of 6240 CsI (Tl) crystals arranged in a cylindrical shape (barrel) plus two endcaps. For 1.0 GeV photons, the energy resolution is 2.5% in the barrel and 5% in the endcaps, and the position resolution is 6 mm in the barrel and 9 mm in the endcaps; 3) a Time-Of-Flight system (TOF) for particle identification composed of a barrel part made of two layers with 88 pieces of 5 cm thick, 2.4 m long plastic scintillators in each layer, and two endcaps with 96 fan-shaped, 5 cm thickness, plastic scintillators in each endcap. The time resolution is 80 ps in the barrel, and 110 ps in the endcaps, corresponding to a K/$\pi$ separation better than a 2 $\sigma$ for momenta below about 1 GeV/$c$; 4) a muon chamber system (MUC) made of 1000 m$^2$ of Resistive Plate Chambers (RPC) arranged in 9 layers in the barrel and 8 layers in the endcaps and incorporated in the return iron of the superconducting magnet. The position resolution is about 2 cm.

The GEANT4-based simulation software BOOST [21] includes the geometric and material description of the BESIII detectors, the detector response and digitization models, as well as the tracking of detector running conditions and performance. $1.06 \times 10^8$ inclusive Monte Carlo (MC) events are used in our background studies. The production of the $\psi(3686)$ resonance is simulated with the event generator KKMC [22, 23], while the decays are generated with EvtGen [24] with known branching fractions [14], and by Lundcharm [25] for unmeasured decays. The analysis is performed in the framework of the BESIII Offline Software System (BOSS) [26] which takes care of the detector calibration, event reconstruction, and data storage.

## III. EVENT SELECTION

In this analysis, the $\omega$ meson is reconstructed in its dominant decay $\omega \to \pi^+\pi^-\pi^0$; $K^0_S$ and $\pi^0$ are reconstructed from the decays $K^0_S \to \pi^+\pi^-$ and $\pi^0 \to \gamma\gamma$. The final states of $\psi(3686) \to \omega K^0_S K^+\pi^-$ and $\omega K^+K^-\pi^0$ are $2(\pi^+\pi^-)K^+\pi^-\gamma\gamma$ and $\pi^+\pi^-K^+K^-\gamma\gamma\gamma\gamma$, respectively[1] .

Charged tracks are reconstructed from MDC hits. Each charged track (except those from $K^0_S$ decays) is required to originate from within 2 cm in the radial direction and 20 cm along the beam direction of the run-by-run-determined interaction point. The tracks must be within the MDC fiducial volume, $|\cos\theta| < 0.93$, where $\theta$ is the polar angle. The information from the TOF and $dE/dx$ is combined to form a probability Prob($K$) (Prob($\pi$) or Prob($p$)) under a kaon (pion or proton) hypothesis. To identify a track as a kaon, Prob($K$) is required to be greater than Prob($\pi$) and Prob($p$).

Electromagnetic showers are reconstructed from clusters of energy deposits in the EMC. The energy deposited in the nearby TOF counters is included to improve the reconstruction efficiency and the energy resolution. A photon

[1] The charge-conjugate final state is included throughout the paper unless explicitly stated.

candidate is a shower in the barrel region ($|\cos\theta| < 0.8$) with an energy larger than 25 MeV, or in the endcap region ($0.86 < |\cos\theta| < 0.92$) larger than 50 MeV, where $\theta$ is the polar angle of the shower. The showers close to the gap between the barrel and the endcap are poorly measured and are thus excluded from the analysis. Moreover, the EMC timing, with respect to the collision, of the photon candidate must be in coincidence with collision events, i.e., $0 \le t \le 700$ ns, to suppress electronic noise and energy deposits unrelated to the event.

$K^0_S$ candidates are reconstructed from secondary vertex fits to all oppositely charged track pairs in an event. The combination with an invariant mass closest to the nominal $K^0_S$ mass ($m_{K^0_S}$) is kept. The reconstructed $K^0_S$ is used as input for the subsequent kinematic fit.

## IV. $\psi(3686) \to \omega K^0_S K^+\pi^- + c.c.$

Event candidates should have a $K^0_S$, four charged tracks with zero net charge, and two or more photons. At least one charged track is positively identified as a kaon. When more than one kaon is identified, the one with the maximum Prob($K$) is chosen. The $\psi(3686) \to \pi^+\pi^- K^0_S K^+\pi^-\gamma\gamma$ candidates are subjected to a four-constraint (4C) kinematic fit provided by four-momentum conservation to reduce background and to improve the mass resolution. For events with more than two photons, the combination with the minimum $\chi^2$ value of the fit (denoted as $\chi^2_{4C}$) is retained, and $\chi^2_{4C}$ is required to be less than 40. For $\pi^0$ candidates formed from a photon pair, the invariant mass of the photon pair must be within the range $|M_{\gamma\gamma} - m_{\pi^0}| < 0.02$ GeV/$c^2$. The combination of $\pi^+\pi^-\pi^0$ with an invariant mass closest to the nominal $\omega$ mass ($m_\omega$) is chosen as an $\omega$ candidate. Figure 1(a) shows the distribution of the $M_{\pi^+\pi^-}$ versus the $M_{\pi^+\pi^-\pi^0}$ invariant mass, where a $\omega - K^0_S$ cluster corresponding to $\psi(3686) \to \omega K^0_S K^+\pi^-$ is apparent. Events are kept for further analysis if the $\pi^+\pi^-$ invariant mass is in the range 0.489 GeV/$c^2$ $< M_{\pi^+\pi^-} <$ 0.505 GeV/$c^2$ and the $\pi^+\pi^-\pi^0$ mass in the range 0.743 GeV/$c^2$ $< M_{\pi^+\pi^-\pi^0} <$ 0.823 GeV/$c^2$. Events in the $K^0_S$ sideband range (0.012 GeV/$c^2$ $< |M_{\pi^+\pi^-} - m_{K^0_S}| <$ 0.02 GeV/$c^2$) or the $\omega$ sideband (0.06 GeV/$c^2$ $< |M_{\pi^+\pi^-\pi^0} - m_\omega| <$ 0.10 GeV/$c^2$) are used to estimate the background. In addition, to veto the $\psi(3686) \to \pi^+\pi^- J/\psi$ background events, the recoil mass against $\pi^+\pi^-$ is required to satisfy $|M^{recoil}_{\pi^+\pi^-} - m_{J/\psi}| > 0.007$ GeV/$c^2$.

### A. Branching fractions for $\psi(3686) \to \omega X(1440) \to \omega K^0_S K^+\pi^- + c.c.$

Figure 1(b) shows the invariant mass $M_{K^0_S K^+\pi^-}$ for selected events, where a peak around 1.44 GeV/$c^2$ (denoted as X(1440), since we do not distinguish $\eta(1405)$ and $\eta(1475)$ from this analysis) and the $f_1(1285)$ are evident. To verify that the observed peaks originate from the process $\psi(3686) \to \omega K^0_S K^+\pi^-$, the backgrounds are investigated from both data sideband and inclusive MC events. The non-$K^0_S$ and non-$\omega$ backgrounds, estimated by using events in the $K^0_S$ and $\omega$ sideband regions, and normalized according to the ratio of MC events falling into the sidebands to the signal region, are shown as the shaded histogram in Fig. 1(b). No evident peak around 1.44 GeV/$c^2$ is seen. Other potential $\psi(3686)$ decay backgrounds are checked with 106 million $\psi(3686)$ inclusive MC events. The main backgrounds come from the decays of $\psi(3686) \to \rho^\pm K^{*\mp} K^{*0} + \rho^0 K^{*\pm} K^{*\mp} \to \pi^\pm\pi^\mp\pi^0 K^0_S K^\pm\pi^\mp$, which do not form a peak in the $M_{K^0_S K^+\pi^-}$ spectrum. The background from the $e^+e^- \to q\bar{q}$ continuum process is studied by using data collected at the center-of-mass energy of 3.65 GeV. Continuum backgrounds are found to be small and uniformly distributed in the mass spectrum.

An unbinned maximum-likelihood fit to $M_{K^0_S K^+\pi^-}$ is applied to determine the number of $\omega X(1440)$ and $\omega f_1(1285)$ events. The fit includes three components: $X(1440)$, $f_1(1285)$, and background. Both $X(1440)$, and $f_1(1285)$ are represented by Breit-Wigner (BW) functions convoluted with a Novosibirsk mass-resolution function [27] and multiplied by an efficiency curve. Both the mass resolution and the efficiency curve are determined from MC simulations. The background shape is described by a 2nd-order Chebychev polynomial function. The mass and width of $f_1(1285)$ are fixed at the known values [14, 28], while those for the $X(1440)$ are allowed to float in the fit. The solid curve in Fig. 1(b) shows the fit results. The goodness-of-fit is $\chi^2/ndf = 81.0/75 = 1.08$, which indicates a reasonable fit. The fit yields $109.2 \pm 18.0$ events for the $X(1440)$ with a statistical significance of $9.5\sigma$, and $21.6 \pm 7.0$ events for the $f_1(1285)$ with the statistical significance of $4.5\sigma$. The significance is determined by the change of the log-likelihood value and the degrees of freedom in the fit with and without assuming the presence of a signal. The mass and width of the $X(1440)$ are determined to be $M = 1452.2 \pm 5.2$ MeV/$c^2$ and $\Gamma = 51.6 \pm 12.1$ MeV/$c^2$. The contribution of background estimated from the sideband is $13.4 \pm 6.1$ for the $X(1440)$ and $0.1 \pm 2.4$ for the $f_1(1285)$. In the analysis, these backgrounds are ignored.

With the MC-determined efficiencies (where the final-state particles distribute uniformly over the phase space) of $(10.41 \pm 0.14)\%$ for $\psi(3686) \to \omega X(1440)$ and $(10.88 \pm 0.15)\%$ for $\psi(3686) \to \omega f_1(1285)$, the products of branching

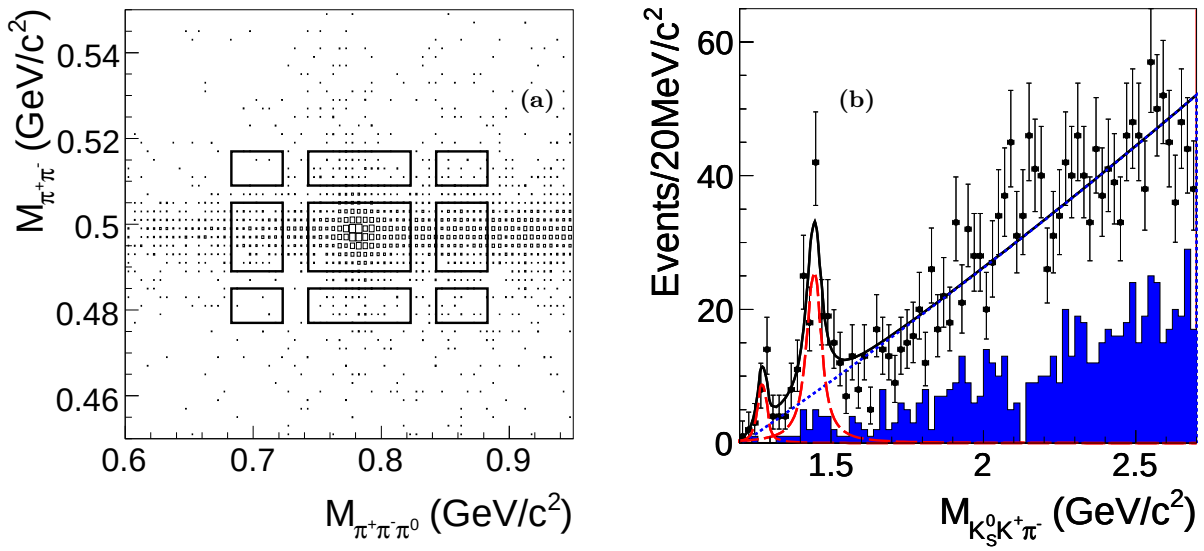


FIG. 1: (a) Distribution of $M_{\pi^+\pi^-}$ versus $M_{\pi^+\pi^-\pi^0}$, where the boxes represent the $K^0_S$ and $\omega$ signal region and sideband regions. (b) The $K^0_S K^+\pi^-$ invariant-mass distribution for $\psi(3686) \to \omega K^0_S K^+\pi^-$ candidate events. The shaded histogram is the background contribution estimated from the $K^0_S$ and $\omega$ sidebands minus that of the corner ranges.

fractions are calculated as listed in Table III. Systematic uncertainties are discussed in more detail in Section VI. Since the $f_1(1285)$ peak is not significant, an upper limit at a 90% confidence level on $N_{sig}$ is determined using a Bayesian method [14] by finding the value $N^{UP}_{sig}$ such that

$$\frac{\int_0^{N^{UP}_{sig}} L dN_{sig}}{\int_0^{\infty} L dN_{sig}} = 0.90,$$

where $N_{sig}$ is the number of signal events, and $L$ is the value of the likelihood as a function of $N_{sig}$. An upper limit at the 90% C.L of 31 $f_1(1285)$ events is obtained. To conservatively estimate the upper limit on the branching fraction for $\psi(3686) \to \omega f_1(1285)(f_1(1285) \to K^0_S K^+\pi^-)$, the systematic error in Table I is considered by dividing by a factor $(1-\delta_{sys})$, where the $\delta_{sys}$ is the systematic error for the decay, and the corresponding upper limit is shown in Table III.

### B. Branching fractions of $\psi(3686) \to \omega K^{*+} K^- + c.c.$ and $\psi(3686) \to \omega \bar{K}^{*0} K^0$

Figure 2 shows the $M_{K^0_S\pi^\pm}$ and $M_{K^\mp\pi^\pm}$ distributions, where the $K^*(892)$ and a peak at 1.43 GeV/$c^2$ are evident in both distributions. The solid lines in Fig. 2 show the results of an unbinned maximum likelihood fit with three components: $K^*(892)$, $K^*_2(1430)$, and background. Both the $K^*(892)$ and $K^*_2(1430)$ are described by acceptance-corrected BW functions. The BW function [29–31] is

$$F_{BW}(s) = \frac{M\Gamma(s)}{(s^2 - M^2)^2 + M^2\Gamma(s)^2}, \quad (1)$$

where $\Gamma(s) = \Gamma(\frac{M}{s})^2(\frac{q}{q_0})^{2L+1}$, $M$ and $\Gamma$ are the $K^*$ mass and width, $q$ is the $K^0_S$ ($K^\mp$) momentum in the $K^*$ rest-frame, $q_0$ is the $q$ value at $s = M$, and $L$ is the relative orbital angular momentum of $K^0_S\pi^\pm$ ($K^\mp\pi^\pm$). Here the $K^*(892)$ and $K^*_2(1430)$ peaks are described with $P$-wave ($L = 1$) and $D$-wave ($L = 2$) BW functions, respectively. The mass and width of the $K^*(892)$ are floating, and those of $K^*_2(1430)$ are fixed to the world average values [14]. The backgrounds are described by the function [32, 33]

$$F_{BG}(s) = (s - m_t)^c e^{-ds-es^2}, \quad (2)$$

where $m_t$ is the threshold mass for $K^0_S\pi^\pm$ ($K^\mp\pi^\pm$) and $c$, $d$ and $e$ are free parameters.

The fit to the $M_{K^0_S\pi^\pm}$ distribution yields $502.0 \pm 56.4$ $K^{*\pm}(892)$ events, and $128.5 \pm 30.0$ $K_2^{*\pm}(1430)$ events with a statistical significance of $4.4\sigma$. The mass and width of the $K^{*\pm}(892)$ determined in the fit are $888.0 \pm 2.5$ MeV/$c^2$ and $48.0 \pm 6.5$ MeV/$c^2$, respectively. The fit to $M_{K^\mp\pi^\pm}$ yields $446.2 \pm 47.4$ $K^{*0}(892)$ events, and $164.2 \pm 34.2$ $K_2^{*0}(1430)$ events with a statistical significance of $4.6\sigma$. The mass and width of the $K^{*0}(892)$ are determined to be $M = 893.9 \pm 2.2$ MeV/$c^2$ and $\Gamma = 45.0 \pm 5.7$ MeV/$c^2$. When the peak at 1430 MeV/$c^2$ is fitted to an $S-$wave $K_0^*(1430)$ or a $P-$wave $K^*(1410)$, the fit qualities degrade for both fits. The $K_2^*(1430)$ can be distinguished from $K_0^*(1430)$ and $K^*(1410)$ with log-likelihood values worse by 173.9 and 173.7, respectively, in the $K^0_S\pi^\pm$ decay, while the log-likelihoods are worse by 170.6 and 169.7, respectively, in the $K^\mp\pi^\pm$ decay.

The peaking backgrounds for $K^*(892)$ and $K_2^*(1430)$ are studied using the $K^0_S$ and $\omega$ sidebands. In $K^0_S\pi^\pm$, the contributions from background events are estimated to be $105.6 \pm 21.6$ for $K^{*\pm}(892)$ while no evident peaking backgrounds for $K_2^{*\pm}(1430)$ are seen; in $K^\mp\pi^\pm$, those are determined to be $90.2 \pm 18.3$ for $K^{*0}(892)$ and $48.5 \pm 23.2$ for $K_2^{*0}(1430)$. Subtracting these background events and combining their detection efficiencies, their corresponding branching fractions of $\psi(3686) \to \omega K^{*+}K^- + c.c.$, $\psi(3686) \to \omega K_2^{*+}(1430)K^- + c.c.$, $\psi(3686) \to \omega \bar{K}^{*0}K^0$ and $\psi(3686) \to \omega \bar{K}_2^{*0}(1430)K^0$ are obtained and summarized in Table IV.

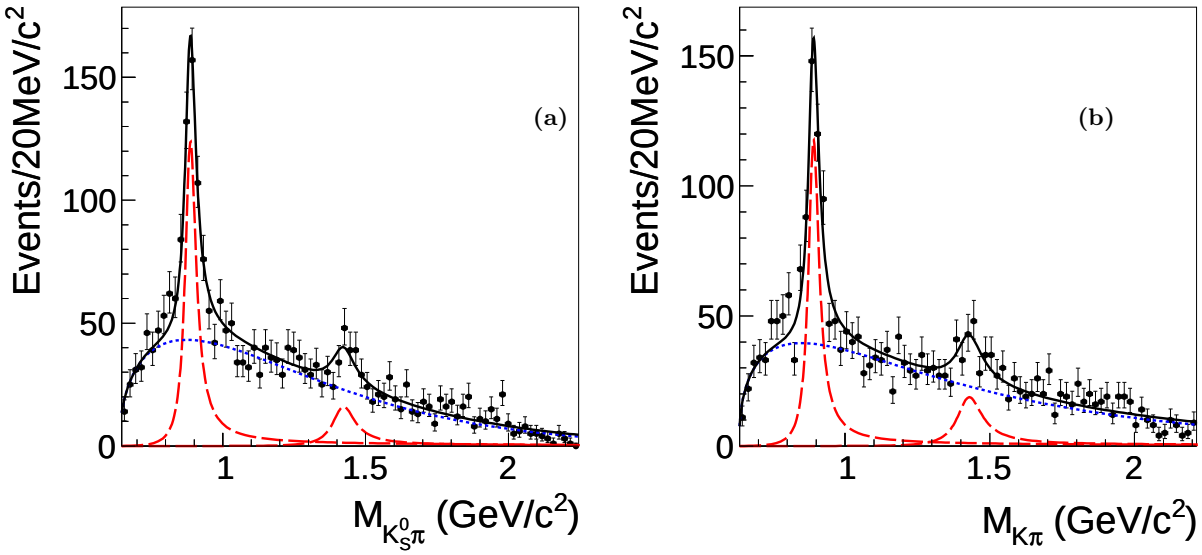


FIG. 2: (a) The $M_{K^0_S\pi^\pm}$ distribution. (b) The $M_{K^\mp\pi^\pm}$ distribution. Solid curves show the fit results; dashed lines are for signals; and dotted lines are for backgrounds.

## V. $\psi(3686) \to \omega K^+K^-\pi^0$

Candidate events must have four charged tracks with zero net charge, and four or more photons. At least two charged tracks should be identified as kaons. When more than two charged tracks are identified as kaons the two oppositely charged tracks with the largest Prob($K$) are chosen. To reject the two backgrounds with $3\gamma$ or $5\gamma$ in the final state, the $\chi^2_{4C}$ of a four-constraint kinematic fit in the hypothesis of $\psi(3686) \to K^+K^-\pi^+\pi^-4\gamma$ is required to be less than those of the $K^+K^-\pi^+\pi^-3\gamma$, and $K^+K^-\pi^+\pi^-5\gamma$ hypotheses. For all possible combinations, a six-constraint kinematic (6C) fit (besides the initial $\psi(3686)$ four-momentum, two $\pi^0$ masses are also used as constraints) is performed, and the one with the least $\chi^2_{6C}$ is chosen, and $\chi^2_{6C} < 100$ is required. The combination of $\pi^+\pi^-\pi^0$ with the invariant mass closest to the nominal $\omega$ mass is selected as an $\omega$ candidate; the invariant mass $M_{\pi^+\pi^-\pi^0}$ must be in the region 0.743 GeV/$c^2$ $< M_{\pi^+\pi^-\pi^0} <$ 0.823 GeV/$c^2$. Background events from $\psi(3686) \to \pi^+\pi^- J/\psi$ and $\psi(3686) \to \pi^0\pi^0 J/\psi$ decays are removed by requiring $|M^{recoil}_{\pi^+\pi^-} - m_{J/\psi}| > 0.007$ GeV/$c^2$ and $|M^{recoil}_{\pi^0\pi^0} - m_{J/\psi}| > 0.06$ GeV/$c^2$. Background events from $\psi(3686) \to \gamma\gamma J/\psi$ are rejected by requiring $|M^{recoil}_{\gamma\gamma} - m_{J/\psi}| > 0.05$ GeV/$c^2$.

### A. Branching fractions for $\psi(3686) \to \omega X(1440) \to \omega K^+K^-\pi^0$

After the above event selection, the distribution of $M_{K^+K^-\pi^0}$ is shown in Fig. 3(a), where the $X(1440)$ is clearly seen and the $f_1(1285)$ is evident. Non-$\omega$ background, estimated from the $\omega$ sideband (0.06 GeV/$c^2$ $< |M_{\pi^+\pi^-\pi^0} - m_\omega| <$ 0.10 GeV/$c^2$), is shown as the shaded histogram and does not form a peak in the $M_{K^+K^-\pi^0}$ spectrum.

The results of an unbinned maximum-likelihood fit to $M_{K^+K^-\pi^0}$, which is similar to the $M_{K^0_SK\pi}$ fit described in Section IV A, is shown as a solid line in Fig. 3. The goodness-of-fit is $\chi^2/ndf = 63.6/67 = 0.95$, which indicates a reasonable fit. The fit yields $81.8 \pm 14.7$ $X(1440)$ events with a statistical significance of $9.3\sigma$, and $9.5 \pm 5.3$ $f_1(1285)$ events with a statistical significance of $3.2\sigma$. The mass and width of the $X(1440)$ determined from the fit are $M = 1452.7 \pm 3.8$ MeV/$c^2$ and $\Gamma = 36.8 \pm 10.5$ MeV/$c^2$, respectively. The non-$\omega$ contributions estimated from the $\omega$ sideband are $2.8 \pm 3.9$ events for the $X(1440)$, and $0.1 \pm 1.5$ events for $f_1(1285)$, which are neglected in the branching fraction measurements. Since the $f_1(1285)$ is not significant, the 90% C.L. upper limit on the number of $f_1(1285)$ events is determined to be 15 with the approach discussed above.

With the detection efficiencies of $(7.92 \pm 0.13)\%$ for $\psi(3686) \to \omega X(1440)$ and $(8.02 \pm 0.13)\%$ for $\psi(3686) \to \omega f_1(1285)$, the corresponding products of branching fractions and upper limit are presented in Table III.

### B. Branching fractions for $\psi(3686) \to \omega K^{*+}K^- + c.c.$

The $M_{K^\pm\pi^0}$ distribution (both $M_{K^+\pi^0}$ and $M_{K^-\pi^0}$ are included) is shown in Fig. 3(b), where the $K^*(892)$ and $K_2^*(1430)$ are clear. Using the same functions as described in Section IV B, an unbinned maximum likelihood fit to $M_{K^\pm\pi^0}$ is performed. The fit yields $678.8 \pm 65.3$ $K^{*\pm}(892)$ and $142.8 \pm 39.0$ $K_2^{*\pm}(1430)$ events with a statistical significance of $4.5\sigma$. The mass and width of $K^{*\pm}(892)$ are determined to be $M = 889.6 \pm 2.1$ MeV/$c^2$ and $\Gamma = 49.2 \pm 5.5$ MeV/$c^2$.

The background contributions from non-$\omega$ processes estimated by fitting $M_{K^\pm\pi^0}$ for events in the $\omega$ sideband are $(144.2 \pm 24.8)$ events for $K^{*\pm}(892)$, which is subtracted from the total $K^{*\pm}(892)$ yield, while no evident peak contributions for $K_2^{*\pm}(1430)$ are present.

With the efficiencies of $(7.48 \pm 0.07)\%$ and $(7.70 \pm 0.07)\%$ for $\psi(3686) \to \omega K^{*+}(892)K^- + c.c.$ and $\psi(3686) \to \omega K_2^{*+}(1430)K^- + c.c.$ determined from MC simulation, their branching fractions are given in Table IV.

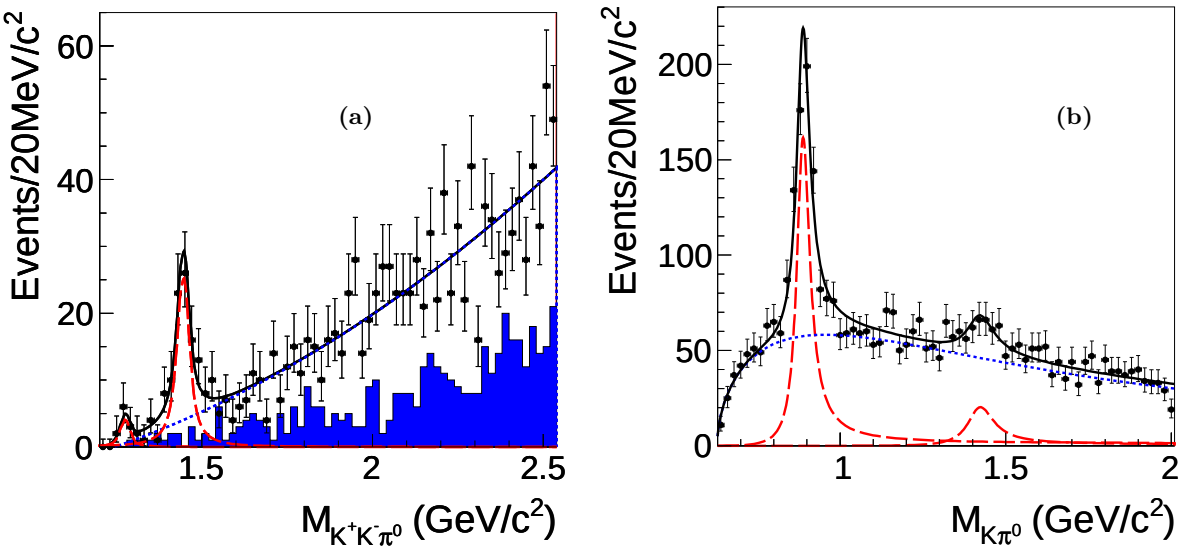


FIG. 3: (a) The $M_{K^+K^-\pi^0}$ invariant-mass distribution for $\psi(3686) \to \omega K^+K^-\pi^0$ candidate events. The shaded histogram is for non-$\omega$ background events estimated from the $\omega$ sideband. (b) The combined mass spectra of $K^+\pi^0$ and $K^-\pi^0$ for $\psi(3686) \to \omega K^{*+}K^-$ candidate events. Solid curves are the fitting results; dashed lines are for the signal; and dotted lines are for the background.

## VI. SYSTEMATIC UNCERTAINTIES

Systematic errors in the branching fraction measurements mainly come from the number of $\psi(3686)$ events, tracking, particle identification, photon reconstruction, $K^0_S$ reconstruction, kinematic fit, background estimation, signal shape and detection efficiency.

The uncertainty on the number of $\psi(3686)$ is 0.81% as reported in Ref. [36]. The tracking efficiencies have been checked with clean channels such as $J/\psi \to \rho\pi$, $J/\psi \to \pi^+\pi^- p\bar{p}$, $\psi(3686) \to \pi^+\pi^- J/\psi$ ($J/\psi \to l^+l^-$) and $J/\psi \to K^{*0}(892)K^0_S$ ($K^{*0} \to K^\pm\pi^\mp$, $K^0_S \to \pi^+\pi^-$). It is found that the MC simulation agrees with data within 1% for each charged track [34]. A 4% systematic error due to the MDC tracking efficiency is assigned for both $\psi(3686) \to \omega K^0_S K^+\pi^-$ and $\psi(3686) \to \omega K^+K^-\pi^0$. The uncertainty associated with the kaon identification has been studied with a clean kaon sample selected from $J/\psi \to K^0_S K^+\pi^-$ [34]. The data-MC efficiency difference, which is 2% per track, is assigned as the systematic error for the kaon identification.

The uncertainty in the $K^0_S$ reconstruction efficiency [35], which includes the geometric acceptance, a pair of pion tracking efficencies and the $K^0_S$ secondary vertex fit, is estimated with the decay of $J/\psi \to K^{*0}K^0$, and the MC-data difference of 3.5% is taken as the systematic error for the $K^0_S$ reconstruction in the decay $\psi(3686) \to \omega K^0_S K^+\pi^-$. The photon detection efficiency is studied with $J/\psi \to \rho^0\pi^0$, and the difference between data and MC simulation is about 1% [34] per photon. A 2% (4%) systematic error for photon efficiency is used for the decay $\psi(3686) \to \omega K^0_S K^+\pi^-$ ($\psi(3686) \to \omega K^+K^-\pi^0$).

The uncertainties associated with the kinematic fit are estimated by using $\psi(3686) \to \pi^+\pi^- J/\psi$ with $J/\psi \to K^0_S K^+\pi^-\pi^0$ or $J/\psi \to K^+K^-\pi^0\pi^0$ events. The efficiencies are obtained by comparing the number of signal events with and without the kinematic fit performed for data and MC simulation separately. A data-MC difference of 5.4% is found in $J/\psi \to K^0_S K^+\pi^-\pi^0$ and 3.2% in $J/\psi \to K^+K^-\pi^0\pi^0$. The differences are taken as the systematic errors.

The uncertainty in the $\mathcal{B}(\psi(3686) \to \omega X(1440))$ measurement due to the background shape is estimated by varying the background function from a 2nd-order polynomial to a 3rd-order polynomial in the fit to $M_{K\bar{K}\pi}$. The changes in $X(1440)$ and $f_1(1285)$ yields, are 5.1% (3.2%) and 2.5% (2.2%), respectively, in the decay $\psi(3686) \to \omega K^0_S K^+\pi^-$ ($\psi(3686) \to \omega K^+K^-\pi^0$). The uncertainty due to the fit range is estimated by repeating the fits in the range [1.2,2.4] GeV/$c^2$, and the differences of 6.1% (3.3%) and 3.3% (6.0%) in the branching fractions for $X(1440)$ and $f_1(1285)$ in the decay $\psi(3686) \to \omega K^0_S K^+\pi^-$ ($\psi(3686) \to \omega K^+K^-\pi^0$) are assigned as systematic errors.

The uncertainty in the $\mathcal{B}(\psi(3686) \to \omega X(1440))$ measurement due to the signal shape is considered to come from the mass resolution, mass shift and phase space factor. By varying the mass resolution by $\pm 0.5$ MeV/$c^2$ from the MC expectation, the differences in $X(1440)$ yield, 1.0% for $K^0_S K^+\pi^-$ and 1.1% for $K^+K^-\pi^0$, are assigned as systematic errors respectively; the difference in the $f_1(1285)$ yield can be ignored. By floating the mass of $f_1(1285)$, the changes, 1.0% for $K^0_S K^+\pi^-$ and 2.1% for $K^+K^-\pi^0$, are taken as the systematic errors. After taking the phase space factor into account, which depends on the momentum of the $X(1440)$ in the $\psi(3686)$ rest frame and the relative orbital angular momentum between the $\omega$ and $X(1440)$, the differences in the fitting results of $X(1440)$ and $f_1(1285)$ are found to be 2.7% and 1.0% in the decay $\psi(3686) \to \omega K^0_S K^+\pi^-$, and 0.5% and 2.1% in the decay $\psi(3686) \to \omega K^+K^-\pi^0$, respectively, which are taken as the uncertainties.

The selection efficiencies are determined from phase space distributed MC simulations of the $\psi(3686)$ decay. The uncertainties in the selection efficiencies are estimated by using efficiencies obtained from MC samples that include intermediate states, or the angular distribution associated with the $X(1440)$. There is a small difference (2.5% for $K^0_S K^+\pi^-$ and 3.2% for $K^+K^-\pi^0$) from the $\bar{K}^*K$ intermediate process. The detection efficiencies are also checked by generating $\psi(3686) \to \omega X(1440)$ MC events assuming X(1440) is a pseudoscalar meson, and the differences for $X(1440) \to K^0_S K^+\pi^-$ and $X(1440) \to K^+K^-\pi^0$ are 10.0% and 11.3%, respectively. To be conservative, the differences of 10.0% and 11.3% are taken as the systematic errors for the $X(1440) \to K^0_S K^+\pi^-$ and $X(1440) \to K^+K^-\pi^0$, respectively.

The uncertainties in the $\mathcal{B}(\psi(3686) \to \omega\bar{K}^*K)$ measurement due to the fit range are estimated to be 7.6% (8.9%), 3.6% (9.1%) and 3.6% (11.6%) for the decay $K^{*\pm}(892)(K^{*\pm}_2(1430)) \to K^0_S\pi^\pm$, $K^{*0}(892)(K^{*0}_2(1430)) \to K^\mp\pi^\pm$ and $K^{*\pm}(892)(K^{*\pm}_2(1430)) \to K^\pm\pi^0$, respectively. The differences by changing the sideband range (0.014 GeV/$c^2$ $< |M_{\pi^+\pi^-} - m_{K^0_S}| <$ 0.022 GeV/$c^2$ or 0.08 GeV/$c^2$ $< |M_{\pi^+\pi^-\pi^0} - m_\omega| <$ 0.12 GeV/$c^2$) are estimated for the above decay modes. For $K^*(892)$, the differences in the fitting results with or without the presence of $K^*_2(1430)$ or by replacing $K^*_2(1430)$ with $K^*_0(1430)$ (or $K^*(1410)$) are also estimated. The above largest differences are taken as the systematic errors of the $K^*(892)$.

All the contributions are summarized in Table I and Table II. The total systematic uncertainty is given by the quadratic sum of the individual errors, assuming all sources to be independent.

TABLE I: The systematic errors (%) of $\mathcal{B}(\psi(3686) \to \omega X \to \omega K\bar{K}\pi)$.

| Sources | $\omega K^0_S K^+\pi^-$ | | $\omega K^+K^-\pi^0$ | |
|---|---|---|---|---|
| | $X(1440)$ | $f_1(1285)$ | $X(1440)$ | $f_1(1285)$ |
| The number $\psi(3686)$ events | 0.8 | | 0.8 | |
| MDC tracking | 4 | | 4 | |
| Particle identification | 2 | | 4 | |
| $K^0_S$ reconstruction | 3.5 | | - | |
| Photon efficiency | 2 | | 4 | |
| Intermediate decays | 0.8 | | 0.8 | |
| Kinematic fit | 5.4 | | 3.2 | |
| Background uncertainty | 6.1 | 3.3 | 3.3 | 6.0 |
| Signal shape | 2.9 | 1.4 | 1.2 | 3.0 |
| MC Eff. Uncertainty | 10.0 | - | 11.3 | - |
| Total | 14.6 | 8.9 | 14.2 | 10.3 |

TABLE II: The systematic errors (%) of $\mathcal{B}(\psi(3686) \to \omega\bar{K}^*K)$.

| Sources | $\omega K^0_S K^+\pi^-$ | | | | $\omega K^+K^-\pi^0$ | |
|---|---|---|---|---|---|---|
| | $K^{*\pm}(892)$ | $K^{*\pm}_2(1430)$ | $K^{*0}(892)$ | $K^{*0}_2(1430)$ | $K^{*\pm}(892)$ | $K^{*\pm}_2(1430)$ |
| The number of $\psi(3686)$ events | 0.8 | | | | 0.8 | |
| MDC tracking | 4 | | | | 4 | |
| Particle identification | 2 | | | | 4 | |
| $K^0_S$ reconstruction | 3.5 | | | | - | |
| Photon efficiency | 2 | | | | 4 | |
| Intermediate decays | 0.8 | | | | 0.8 | |
| Kinematic fit | 5.4 | | | | 3.2 | |
| Background uncertainty | 7.6 | 8.9 | 3.6 | 9.1 | 7.2 | 11.6 |
| Total | 11.2 | 12.1 | 9.0 | 12.3 | 10.6 | 14.0 |

## VII. DISCUSSION

As the $X(1440)$ and $f_1(1285)$ are observed in both $K^0_S K^\pm\pi^\mp$ and $K^+K^-\pi^0$ final states, a simultaneous maximum-likelihood fit is performed to the mass spectra to extract a more precise determination of the resonant parameters and branching fractions. The fit includes three components, the $X(1440)$, $f_1(1285)$, and background, as used in the fit to each individual mode in Section IV A and Section V A. The fit, shown in Fig. 4, has a $\chi^2/ndf = 72.9/70 = 1.04$, and the statistical significances of the $X(1440)$ and $f_1(1285)$ are $13.3\sigma$ and $5.4\sigma$, respectively. The mass and width of the $X(1440)$ from the fit are $M = 1452.7 \pm 3.3$ MeV/$c^2$ and $\Gamma = 45.9 \pm 8.2$ MeV/$c^2$. The yields of the $X(1440)$ events are $111.4 \pm 17.2$ in the $K^0_S K^\pm\pi^\mp$ mode and $82.4 \pm 13.5$ in the $K^+K^-\pi^0$ mode, while those of the $f_1(1285)$ events are $23.1 \pm 7.1$ in the $K^0_S K^\pm\pi^\mp$ mode and $8.7 \pm 4.6$ in the $K^+K^-\pi^0$ mode, in good agreement with the separate fits to the two modes, as shown in Table III. Combining the observed numbers of signal events with efficiencies and taking properly into account the Clebsch-Gordan coefficients, the branching fractions are

$$\mathcal{B}(\psi(3686) \to \omega X(1440)) \cdot \mathcal{B}(X(1440) \to K\bar{K}\pi) \;=\; (5.48 \pm 0.61\ (\text{stat.}) \pm 0.86\ (\text{sys.})) \times 10^{-5},$$

and

$$\mathcal{B}(\psi(3686) \to \omega f_1(1285)) \cdot \mathcal{B}(f_1(1285) \to K\bar{K}\pi) \;=\; (8.78 \pm 2.33\ (\text{stat.}) \pm 0.96\ (\text{sys.})) \times 10^{-6}.$$

The first errors are statistical and the second ones systematic. In calculating the systematic errors, the correlations between the errors in the two modes shown in Table I are properly taken into account.

To examine the spin-parity of the events at around 1.4 GeV/$c^2$, we try to measure the polar angle distribution (denoted as $\cos\theta_X$) of the $X(1440)$ in the $\psi(3686)$ rest frame. The $|\cos\theta_X|$ distribution is divided into five bins in the region of $[0, 1]$. In each bin, the combined $K\bar{K}\pi$ mass spectrum of the two decay modes is fitted. For $X(1440)$, the mass and width are fixed to those of the combined mass spectrum fitting for the whole angular range; for $f_1(1285)$, the mass and width are fixed at the known values. By repetition of the mass fit in five bins of $|\cos\theta_X|$, the number of $X(1440)$ events can be obtained. Figure 5 shows the polar angular distribution for signal yields, where the errors are statistical only.

The angular distribution is fitted to $1 + \alpha\cos^2\theta_X$, as shown in the solid line in Fig. 5, and $\alpha = 0.58 \pm 0.64$ is obtained with a probability of 29%. Around 1.44 GeV/c$^2$, there are two known resonances, namely the $\eta(1440)$ with

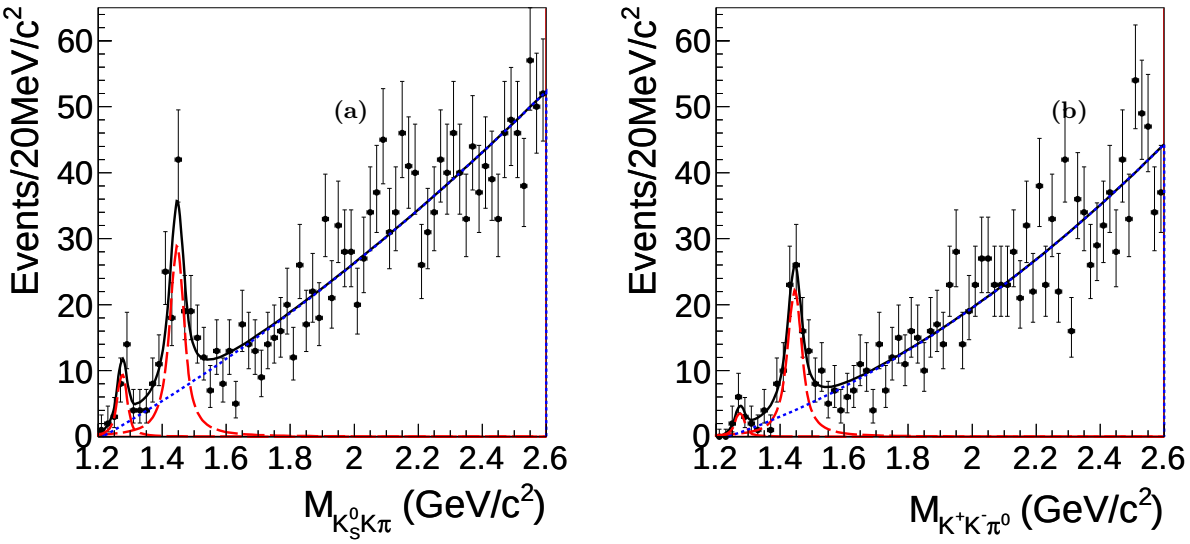


FIG. 4: The simultaneous maximum-likelihood fit to the mass spectra for $K^0_S K^{\pm}\pi^{\mp}$ (a) and $K^+K^-\pi^0$ (b). Points with error bars are data, and the curves show the best fits.

$J^{PC} = 0^{-+}$ and the $f_1(1420)$ with $J^{PC} = 1^{++}$ [14]. The present statistics are not sufficient to establish a $1+\cos^2\theta_X$ behavior as a pseudoscalar meson candidate of $\eta(1440)$, but the data clearly favor $\alpha = 1$ or $\alpha = 0$ over $\alpha = -1$, as can be seen from Fig. 5.

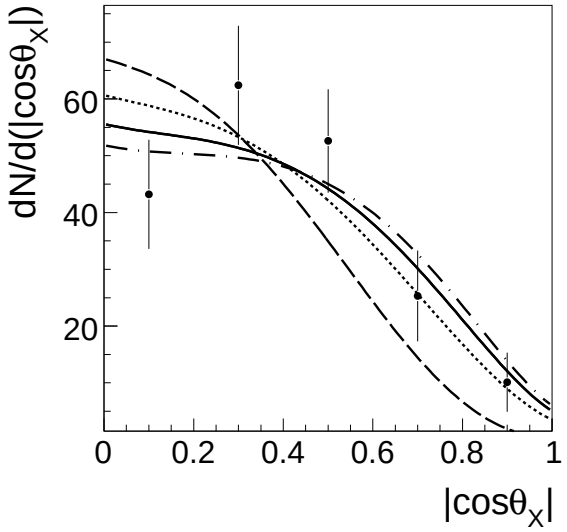


FIG. 5: The $|\cos\theta_X|$ distribution with the fit results; solid line is for $1+\alpha\cos^2\theta_X$ with $\alpha = 0.58 \pm 0.64$; dash-dotted line is for $1+\cos^2\theta_X$; dotted line is for $1+0\cdot\cos^2\theta_X$; and dashed line is for $1-\cos^2\theta_X$. The expectation distributions are multiplied by the efficiency.

## VIII. SUMMARY

With a sample of 106 million $\psi(3686)$ events, the decay of $\psi(3686) \to \omega K\bar{K}\pi$ is studied for the first time. In addition to the mass enhancement ($X(1440)$) around 1.44 GeV/$c^2$, the $f_1(1285)$ is observed in the mass spectrum of

TABLE III: The branching fractions and upper limits (90% C.L.) for $\psi(3686) \to \omega X \to \omega K\bar{K}\pi$ decays. Results for corresponding $J/\psi$ decays [37] and the ratio $Q_h = \frac{\mathcal{B}(\psi(3686)\to h)}{\mathcal{B}(J/\psi\to h)}$ are also given.

| decay mode | $N_{sig}$ | $\epsilon(\%)$ | $\mathcal{B}(\psi(3686))(\times10^{-5})$ | $\mathcal{B}(J/\psi)(\times10^{-5})$ | $Q_h(\%)$ |
|---|---|---|---|---|---|
| $\omega X(1440) \to \omega K_S^0 K^+\pi^-$ | $109 \pm 18$ | $10.41 \pm 0.14$ | $1.60 \pm 0.27 \pm 0.24$ | $48.6 \pm 6.9 \pm 8.1$ | $3.3 \pm 1.1$ |
| $\to \omega K^+K^-\pi^0$ | $82 \pm 15$ | $7.92 \pm 0.13$ | $1.09 \pm 0.20 \pm 0.16$ | $19.2 \pm 5.7 \pm 3.8$ | $5.7 \pm 2.5$ |
| $\to \omega K\bar{K}\pi$ | ... | ... | $5.48 \pm 0.61 \pm 0.86$ | ... | ... |
| $\omega f_1(1285) \to \omega K_S^0 K^+\pi^-$ | $21.6 \pm 7.0$ | $10.88 \pm 0.15$ | $0.302 \pm 0.098 \pm 0.027$ | ... | ... |
| | $< 31$ | $10.88 \pm 0.15$ | $< 0.478$ | ... | ... |
| $\to \omega K^+K^-\pi^0$ | $9.5 \pm 5.3$ | $8.02 \pm 0.13$ | $0.125 \pm 0.070 \pm 0.013$ | ... | ... |
| | $< 15$ | $8.02 \pm 0.13$ | $< 0.221$ | ... | ... |
| $\to \omega K\bar{K}\pi$ | ... | ... | $0.878 \pm 0.233 \pm 0.096$ | ... | ... |

TABLE IV: The branching fractions of $\psi(3686) \to \omega\bar{K}^*K$.

| decay mode | $N_{sig}$ | $\epsilon(\%)$ | $\mathcal{B}(\psi(3686))(\times10^{-5})$ | $\mathcal{B}(J/\psi)(\times10^{-5})$ | $Q_h(\%)$ |
|---|---|---|---|---|---|
| $\omega K^{*+}(892)K^- \to \omega K_S^0 K^+\pi^-$ | $396.4 \pm 60.4$ | $9.58 \pm 0.08$ | $18.9 \pm 2.9 \pm 2.2$ | $310 \pm 34 \pm 56$ | $6.1 \pm 1.8$ |
| $\to \omega K^+K^-\pi^0$ | $534.6 \pm 69.9$ | $7.48 \pm 0.07$ | $22.6 \pm 3.0 \pm 2.4$ | $327 \pm 51 \pm 68$ | $7.0 \pm 2.2$ |
| $\omega K_2^{*+}(1430)K^- \to \omega K_S^0 K^+\pi^-$ | $128.5 \pm 30.0$ | $9.18 \pm 0.07$ | $6.39 \pm 1.50 \pm 0.78$ | ... | ... |
| $\to \omega K^+K^+\pi^0$ | $142.8 \pm 39.0$ | $7.70 \pm 0.07$ | $5.86 \pm 1.61 \pm 0.83$ | ... | ... |
| $\omega \bar{K}^{*0}(892)K^0 \to \omega K_S^0 K^+\pi^-$ | $356.0 \pm 50.8$ | $9.66 \pm 0.08$ | $16.8 \pm 2.5 \pm 1.6$ | $310 \pm 34 \pm 56$ | $5.4 \pm 1.5$ |
| $\omega \bar{K}_2^{*0}(1430)K^0 \to \omega K_S^0 K^+\pi^-$ | $115.7 \pm 41.3$ | $9.08 \pm 0.07$ | $5.82 \pm 2.08 \pm 0.72$ | ... | ... |

$K\bar{K}\pi$. From investigating the $X(1440)$ polar angle distribution, the present statistics are not sufficient to establish a $1 + \cos^2\theta_X$ behavior as a pseudoscalar meson candidate of $\eta(1440)$, but the data favor $\alpha = 1$ or $\alpha = 0$ over $\alpha = -1$. The product branching fraction upper limit of $f_1(1285)$ in each individual mode is also presented Also the branching fractions of $\psi(3686) \to \omega\bar{K}^*K$ for the charged and neutral mode are measured for the first time. The observed $K^*(1430)$ favors $K_2^*(1430)$ over $K_0^*(1430)$ and $K^*(1410)$. The numbers of observed events, detection efficiencies and branching fractions (or upper limits) are summarized in Tables III and IV.

To compare with the 12% rule, Tables III and IV also include the corresponding $J/\psi$ branching fractions [37], as well as the ratio $Q_h$. The data show that $\psi(3686)$ decaying into $\omega X(1440)$ and $\omega\bar{K}^*(892)K$ are suppressed by a factor of $2-4$.

## IX. ACKNOWLEDGEMENT

The BESIII collaboration thanks the staff of BEPCII and the computing center for their hard efforts. This work is supported in part by the Ministry of Science and Technology of China under Contract No. 2009CB825200; National Natural Science Foundation of China (NSFC) under Contracts Nos. 10625524, 10821063, 10825524, 10835001, 10935007, 11125525, 11235011; Joint Funds of the National Natural Science Foundation of China under Contracts Nos. 11079008, 11179007; the Chinese Academy of Sciences (CAS) Large-Scale Scientific Facility Program; CAS under Contracts Nos. KJCX2-YW-N29, KJCX2-YW-N45; 100 Talents Program of CAS; German Research Foundation DFG under Contract No. Collaborative Research Center CRC-1044; Istituto Nazionale di Fisica Nucleare, Italy; Ministry of Development of Turkey under Contract No. DPT2006K-120470; U. S. Department of Energy under Contracts Nos. DE-FG02-04ER41291, DE-FG02-94ER40823; U.S. National Science Foundation; University of Groningen (RuG) and the Helmholtzzentrum fuer Schwerionenforschung GmbH (GSI), Darmstadt; WCU Program of National Research Foundation of Korea under Contract No. R32-2008-000-10155-0.

[1] G. S. Abrams *et al.*, Phys. Rev. Lett. **33**, 1453 (1974).
[2] W. Tanenbaum *et al.* (MARKI Collaboration), Phys. Rev. D **17**, 1731 (1978).
[3] M. E. B. Franklin *et al.* (MARKII Collaboration), Phys. Rev. Lett. **51**, 963 (1983).
[4] M. Ablikim *et al.* (BES Collaboration), Phys. Lett. B **614**, 37 (2005).
[5] M. Ablikim *et al.* (BES Collaboration), Phys. Rev. D **73**, 052004 (2006).
[6] R. A. Briere *et al.* (CLEO Collaboration), Phys. Rev. Lett. **95**, 062001 (2005).
[7] Y. F. Gu *et al.*, Phys. Rev. D **63**, 114019 (2001).

[8] X. H. Mo *et al.*, HEP&NP **31**, 686 (2007).
[9] N. Brambilla *et al.* (Quarkonium Working Group), Eur. Phys. J. C **71**, 1534 (2011).
[10] Q. Wang *et al.*, Phys. Rev. D **85**, 074015 (2012).
[11] T. Appelquist *et al.*, Phys. Rev. Lett. **34**, 43 (1975).
[12] A. De Rujula *et al.*, Phys. Rev. Lett. **34**, 46 (1975).
[13] P. H. Baillon *et al.*, NC **50A**, 393 (1967).
[14] J. Beringer *et al.* (Particle Data Group), Phys. Rev. D **86**, 010001 (2012).
[15] M. Acciarri *et al.* (L3 Collaboration), Phys. Lett. B **501**, 1 (2001).
[16] R. Ahohe *et al.* (CLEO Collaboration), Phys. Rev. D **71**, 072001 (2005).
[17] M. Ablikim *et al.* (BESIII Collaboration), Nucl. Instrum. Meth. A **614**, 345 (2010).
[18] J. Z. Bai *et al.* (BES Collaboration), Nucl. Instrum. Meth. A **344**, 319 (1994).
[19] J. Z. Bai *et al.* (BES Collaboration), Nucl. Instrum. Meth. A **458**, 627 (2001).
[20] "Physics at BESIII", Edited by K. T. Chao and Y. F. Wang, Int. J. Mod. Phys. A **24**, No. 1 (2009) supp.
[21] Z.Y. Deng *et al.*, Chinese Phys. C **30**, 371 (2006).
[22] S. Jadach *et al.*, Phys. Commun. **130**, 260 (2000).
[23] S. Jadach *et al.*, Phys. Rev. D **63**, 113009 (2001).
[24] R.G. Ping *et al.*, Chinese Phys. C **32**, 599 (2008).
[25] J.C. Chen *et al.*, Phys. Rev. D **62**, 034003 (2000).
[26] W.D. Li *et al.*, The Offline Software for the BES-III Experiment, Proceeding of CHEP 2006.
[27] The Novosibirsk function is defined as: $N(m) = A_S \exp(-0.5\{\ln^2[1 + \Lambda\tau \cdot (m - m_0)]/(2\tau^2) + \tau^2\})$ where $\Lambda = \sinh(\tau\sqrt{\ln 4})/(\sigma\tau\sqrt{\ln 4})$, $m_0$ is the peak position, $\sigma$ is the width and $\tau$ is the tail parameter.
[28] M. Ablikim *et al.* (BESIII Collaboration), Phys. Rev. Lett. 107, 182001 (2011).
[29] Matthias Jamin *et al.*, Phys. Lett. B **664**, 78 (2008).
[30] D. Epifanow *et al.* (Belle Collaboration), Phys. Lett. B **654**, 65 (2007).
[31] L. Montanet *et al.* (KLOE Collaboration), Phys. Lett. B **561**, 55 (2003).
[32] C. C. Chang *et al.*, Phys. Rev. D **29**, 1888 (1984).
[33] D. Barberis *et al.* (WA102 Collaboration), Phys. Lett. B **436**, 204 (1998).
[34] M. Ablikim *et al.* (BESIII Collaboration), Phys. Rev. D **83** 112005 (2011).
[35] M. Ablikim *et al.* (BESIII Collaboration), Phys. Rev. Lett. **109**, 042003 (2012).
[36] M. Ablikim *et al.* (BESIII Collaboration), arXiv:1209.6199.
[37] M. Ablikim *et al.* (BES Collaboration), Phys. Rev. D **77**, 032005 (2008).